Design and Analysis of Low Cost Electro-dermal Response System Using Texas Instrument's MSP430 Value Line Launchpad

Sumanth Reddy Yeddula, Gleb V. Tcheslavski[*]

Drayer department of Electrical Engineering
Lamar University
PO Box 10029, Beaumont, TX, 77710, USA
E-mails: sumanthreddy.y@gmail.com, gleb@lamar.edu

[*]*Corresponding author*

Abstract: *Electro-dermal Response (EDR) is one of the important bioelectric signals used in various applications and research studies in the multitude of disciplines, such as Psychophysiology and other areas of Neuroscience. In present paper, a low cost EDR system is designed using Texas Instrument's MSP430 Value Line Launchpad with a general potential divider circuit as the EDR sensor.*

Throughout this paper, much emphasis is laid out on developing an inexpensive system that shall be easily affordable while offering quality measurements. The system is well incorporated to have a decently accurate and fast data acquisition system, good communication capability with PC for storage and analysis. The developed prototype was used in performing two experiments related to the effects of Deep Breath and Visual Stimulus on EDR data, which gave substantiating results as per the theory.

Keywords: *Electro-dermal response, MSP430, Microcontroller, Moving-average filter, Arousal, Emotions.*

Introduction

Electro-dermal Response (EDR) is one of the most important bio-electric signals that can be easily measured and, therefore, is widely used in studies of physiological and psychological activities. EDR is the estimate of electrical conductivity of the skin, which is an indirect measure of the sweat gland activity, which may be affected by various physiological and psychological factors.

Neumann and Blanton presented a detailed history of electro-dermal research [14]. Malmivuo and Plonsey discussed the physiology of the skin and relation of EDR to the autonomous nervous system [13]. Also, EDR is widely used in studies of underlying functioning of Peripheral Sympathetic System and, as a result, it is regarded as Peripheral Autonomic Surface Potential in clinical Neurophysiological literature [2, 9].

Although the underlying fundamentals of EDR are yet to be clarified, this phenomenon is widely used in various applications ranging from polygraphs [30] to psychological treatments, such as hypnotherapy [3], etc. It is also used in the analysis and treatment of emotional disorders, stress-related disorders, etc. [22]. EDR is widely used as one of the key measurements for Biofeedback monitoring [20, 21]. It is pronounced as the best and inexpensive psychophysiological index used to study the emotional and cognitive states of the brain [3, 6, 10, 11, 27].

EDR can be measured using skin resistance, skin conductance, endosomatic potential, etc. [2]. Cornell students, as a part of their course work, built a circuit to estimate EDR that uses an amplifier and filters to evaluate skin conductance [28]. Although a galvanometer circuit based measurement of Electro Dermal activity is an old technique, it is still in use in various polygraph devices [7, 30]. Few modern circuits use stages of OP-AMPS for signal conditioning. Recently, a wearable EDR-based device named Q-sensor was introduced by Affectiva Inc. to analyze human emotions in both commercial and research applications [1, 16].

In the present paper, EDR is evaluated as an exosomatic potential evaluated in terms of the resistance or conductance of the skin between two points. We propose using the concept of potential divider circuit powered by a DC source, unlike the well-defined conventional ways of measuring electro-dermal activity using either constant current or voltage sources and constant effective voltage or effective current for DC and AC methods respectively [2, 7, 13]. Our goal was to build a device prototype that would be of low-cost, yet sufficiently accurate and can be used in the academic research with due safety precautions.

Texas Instruments Inc. has released a low cost hobbyist, academic MSP430 Launchpad Value Line Development Kit [24]. With the cost around 10 USD, it is widely used in variety of applications, such as for building low cost ECG acquisition systems [8]. The kit supports 16-bit high performance and low power MSP430 family microcontrollers and is shown in Fig. 1.
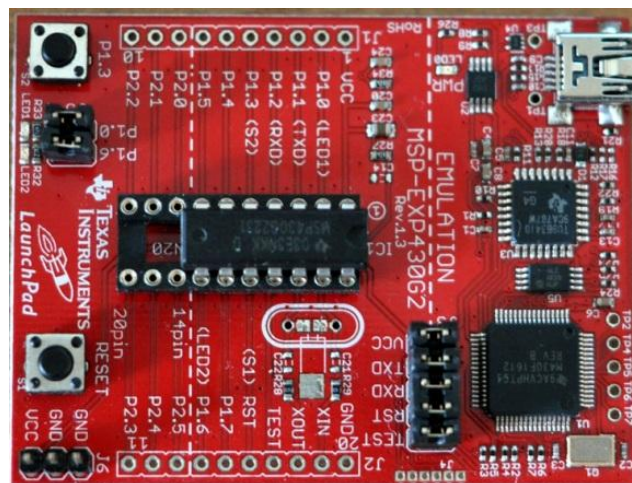

Fig. 1 An image of Texas Instruments MSP430 Launchpad Value
Line Development Kit with MSP430G2231 MCU installed

The MSP430 value line microcontrollers generally incorporate 10-Bit ADC that may be used in a data acquisition system.

EDR variations

Based on various stimuli, ambient conditions, and other factors, the sweat gland activity changes with the physical and mental activities of the body; therefore, affecting the EDR. According to literature, skin resistance tends to be higher when the subject is in a relaxed state compared to the stressful state [13, 29].

The value of skin resistance changes from subject to subject even under the similar conditions as it is dependent on the subject's properties, such as the thickness of the epidermal layer, sweat gland sensitivity, etc. In general, the skin resistance ranges between 1 kΩ and 1 MΩ [5, 29].

It has been shown that deep breathing and various emotional states affect the sweat gland activity and, therefore, EDR [5]. Fig. 2 illustrates representation of Emotion using arousal-valence model.
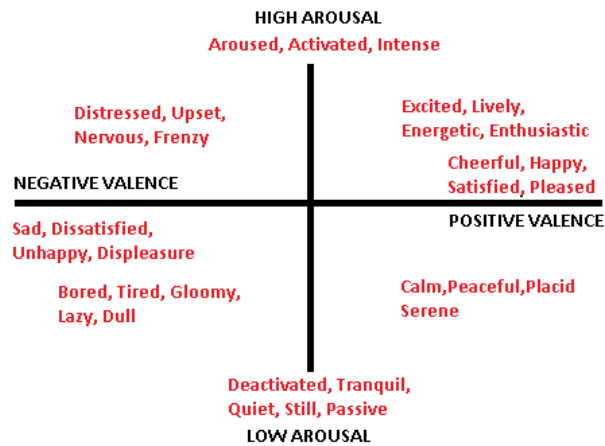

Fig. 2 Arousal-Valence model representation of emotions [27]

It is seen in Fig. 2 that to understand the emotional state of a subject, it is necessary to have information about both the valence and the arousal where the former describes the type of the emotion and the latter describes the magnitude of the activity. For example, a subject can be aroused with excitement or aroused with fear. In either case, subject is emotionally aroused but having a negative valence in case of fear and a positive valence in case of joyous excitement. It is important to note that valence part of the emotion cannot be recognized with EDR. Only the arousal part of the emotion influences the EDR [6, 7, 11, 27, 29]. The emotional state of the subject can be determined using EDR to detect the arousal. Other complementary physiological measurements such as facial expressions [1], EMG, ECG, and Respiratory Signal [6, 11, 27] etc., may be employed to detect valence. Based on the latter, two experiments were established to test the designed EDR system.

Methods: design of a Launchpad-based EDR system

The main objective of the project was to design a low cost EDR acquisition system and store the acquired data on the Personal Computer for further analysis. Therefore, authors emphasize on the design of an EDR sensor using general passive circuit components that can be built without involving much cost. An interface system for communications between PC and the kit has been developed. Matlab was used for the analysis of EDR in the present work. The design of EDR sensor with suboptimal external resistance, Microcontroller programming, system interface design, and future improvements that can be incorporated into this Launchpad-based EDR system are discussed next.

High-level system design

Fig. 3 presents the general high-level block-diagram of the EDR system, while the design details of each block are discussed in the subsequent sections.
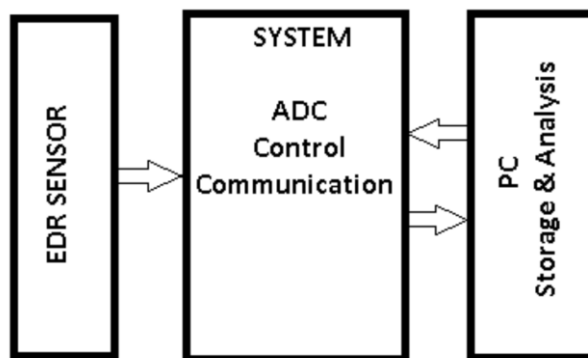
Fig. 3 A block diagram of high-level system design

The first block is the EDR sensor, which is placed on the subject's hand to evaluate EDR. The measured EDR is passed to Launchpad for further conversion to a digital signal. The Launchpad Kit is used as the SYSTEM module or the second block shown in Fig. 3. It includes the built-in circuits and necessary microcontroller to implement the ADC, control, and communication. MSP430G2231 microcontroller was used with the kit [25, 26].

The kit is connected to a PC through a USB protocol, supplying the kit with the power needed. The same *Vcc* of the kit is used to power EDR sensor circuit. As USB on PC is isolated from hazardous high voltages, the prototype is safe to experiment on human subjects (although it is not approved for medical practice). Also, the included external resistor in the EDR sensor limits the short circuit current when the skin resistance drops dramatically.

The onboard UART-based USB communication is used for data exchange between PC and Launchpad. A control program running on PC and microcontroller coordinates and controls the data acquisition process. A workstation running windows 7 with 2 GB RAM, Intel Core 2 Duo processor, 80 GB of internal HDD and with few USB ports is used as the PC – the third block shown in Fig. 3. Code Composer Studio installed on a PC was used to program and debug the microcontroller on Launchpad.

EDR sensor design
In this paper, EDR sensor is designed as a generic potential divider circuit without using any signal conditioning OP-AMP stages as shown in Fig. 4.
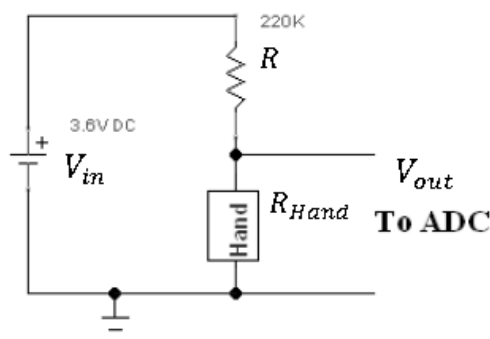

Fig. 4 A circuit diagram of the potential divider used in EDR sensor and powered by 3.6 V DC source (*Vcc* of Launchpad)

The functionality of the EDR sensor is based on the exosomatic measurement of skin resistance between two points on the hand corresponding to R_{hand} in the Fig. 4. R represents the external resistance.

Although a similar circuit was earlier used to measure EDR for emotion recognition in Advanced Multimodal Biometric Emotion Recognition (AMBER) system, EDR sensor circuit design details were not thoroughly discussed and verified while building the AMBER system [10]. In this paper, a detailed discussion on selection of a sub-optimal external resistance is presented in the next subsection.

Two metallic ring electrodes are used and placed on the Distal Phalanx and Medial Phalanx of the index finger as shown in Fig. 5.
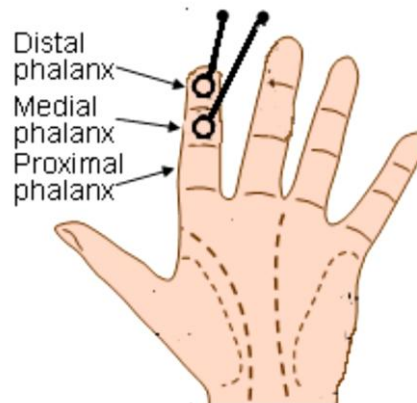

Fig. 5 The electrode placement on the index finger
of the left hand with palm facing towards subject [17]

Generally, in earlier EDR systems, electrodes were placed on Medial phalanx of index and middle finger. As seen in Fig. 5, the placement of one of the electrodes is chosen on Distal Phalanx to take the advantage of increased reactivity of Distal Phalanx [19]. Therefore, Distal Phalanx electrode helps to improve the overall sensitivity of the EDR sensor.

Sub-optimal value of external resistance R
In present project, the EDR sensor circuit was implemented as a generic potential divider circuit shown in Fig. 4. The two points on the hand measuring R_{hand} are considered as an unknown resistance that is in series with a known external resistance R. The circuit is driven by a DC voltage source. Based on the variations in the subjects' state, the EDR varies, producing changes of skin resistance and, as a result, variations in the voltage across the hand may be observed. The registered voltage across the hand is sent to an ADC of microcontroller for the data acquisition. The voltage output across the hand, V_{out} can be expressed as follows:

$$V_{out} = \frac{R_{hand} V_{in}}{R_{hand} + R} \tag{1}$$

where V_{in} is the DC voltage source that drives the circuit, R_{hand} and R are the unknown hand resistance and the reference (known) external resistance, respectively.

Since the Launchpad powers the EDR sensor, $V_{in} = 3.6$ V. The ADC of microcontroller has the same voltage as reference for conversion purposes.

Also, since a 10 bit ADC is implemented, 1024 distinct values of voltage are possible (0x000-0x3FF in Hexadecimal or 0-1023 in Decimal). 0x000 is observed for $V_{out} = 0$; when the voltage is measured across a short circuit in place of R_{hand}. Similarly, 0x3FF is measured for an open circuit where $V_{out} = V_{in}$. An analog factor n is defined such that it equals the ratio of V_{out} to V_{in} and has a range of 0 to 1:

$$n = \frac{V_{out}}{V_{in}} = \frac{R_{hand}}{R_{hand} + R} \tag{2}$$

The above equation generalizes and normalizes the calculations, thereby making them independent of both V_{in} that is the ADC reference voltage and the EDR sensor source voltage. ADC output is denoted as *OUT* and has a range from 0 to 1023. It can be expressed as:

$$OUT = floor(1024n) \tag{3}$$

where *floor* indicates the rounding towards -∞ operation. Knowing *OUT*, R_{hand} can be estimated as follows:

$$R_{hand} = \frac{OUT \, R}{1024 - OUT} = R \frac{n}{1-n} \tag{4}$$

R_{hand} generally varies between 1 kΩ and 1 MΩ. When sweat gland activity causes to hydrate the skin during normal conditions, R_{hand} varies from 50 kΩ to 100 kΩ. On the other hand, during emotionally activated condition, R_{hand} may reduce below 50 kΩ [29].

The value of external resistance R is selected so that the ADC output should be approximately linear and have a maximum range corresponding to R_{hand} varying from 50 kΩ to 1 MΩ. The sub-optimal algorithm satisfying the maximum range of n for a known variation in R_{hand} was implemented in Matlab and the following Fig. 6 was obtained.
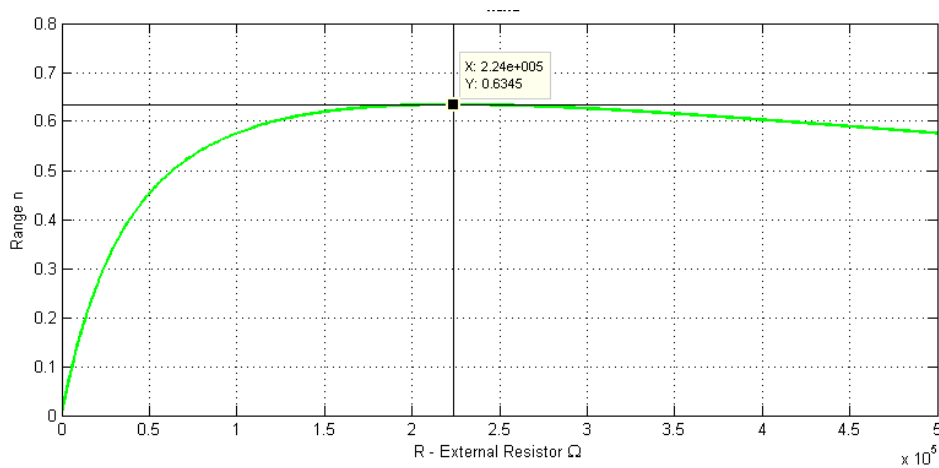

Fig. 6 Range n vs R for R_{hand} 50 kΩ ÷ 1 MΩ. The maximum range is possible for $R = 224$ kΩ.

It is evident from Fig. 6 that $R = 224$ kΩ is the value satisfying both the linearity and range constraints. The nearest standard value available $R = 220$ kΩ was used and the EDR sensor circuit was implemented. Using Matlab, the approximate behavior of ADC coupled with the EDR sensor was analyzed in terms of ADC Output OUT and the results are shown in Fig. 7 and Fig. 8.
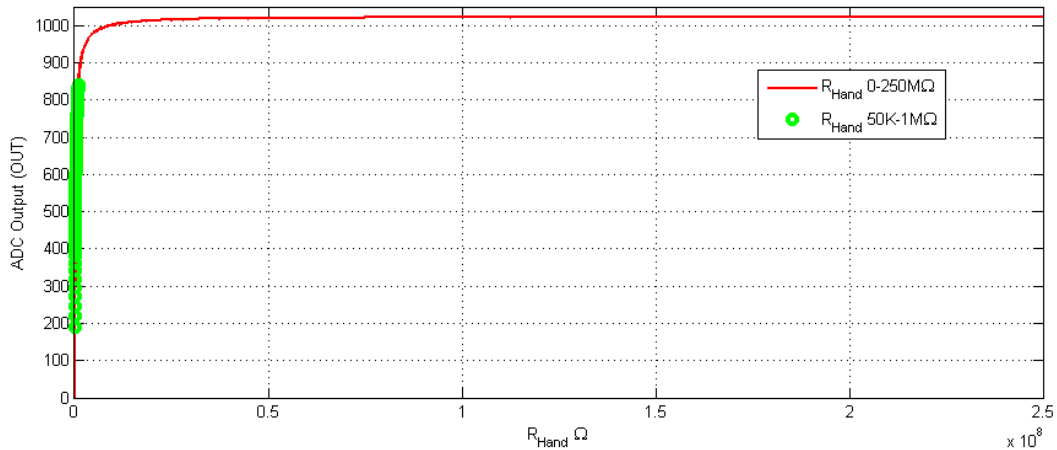
Fig. 7 ADC Output *OUT* as a function of R_{hand} for R = 220 KΩ

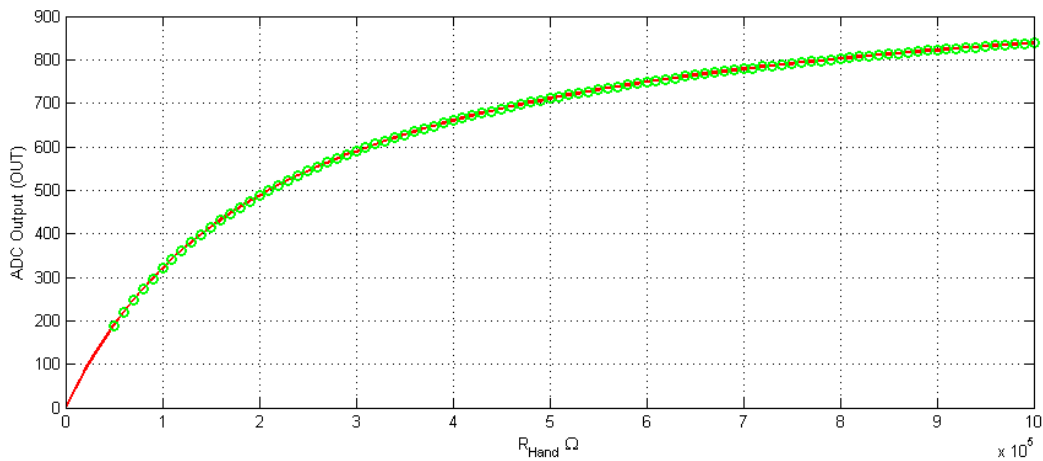Fig. 8 ADC output *OUT* as a function of R_{hand} for R = 220 kΩ: zoomed-in version

As seen in Fig. 7, a continuous line indicates the ADC output *OUT* having a range of 0-1023 where R_{hand} varies from 0 to 250 MΩ. The "o" points in the plot indicate the ADC output *OUT* for a limited range where R_{hand} varies from 50 kΩ to 1 MΩ. Also, it is evident from Fig. 7, that ADC output *OUT* is approximately linear for R_{hand} varying from 50 kΩ to 1 MΩ compared to the overall range.

Although appearing as linear in Fig. 7, Fig. 8 showing a zoomed-in resistance range from 50 kΩ to 1 MΩ reveals a considerable non-linearity in the ADC output.

Microcontroller programming and system interface
While programming the ADC, sample-hold process cycle time was chosen as 64 cycles of internal ADC clock set to a frequency of 5/8 MHz, such that the internal sample-hold circuit capacitor charges to the V_{out} [25, 26].

Universal Serial Interface (USI) based communication is supported by MSP430G2231 microcontroller device [16]. The microcontroller was programmed to communicate with PC via Launchpad's UART based USB protocols. Launchpad has a default Microsoft windows driver that treats the USB interface as a virtual COM port and communicates with the Launchpad at a 9600 baud rate. A Python program [17] using pyserial API was used as the interface controlling the acquisition process [16]. The interface program reads the data sent to

PC by the Launchpad and stores it in a file for further processing and analysis. The interface program was designed implementing the state level transition diagram shown in Fig. 9.
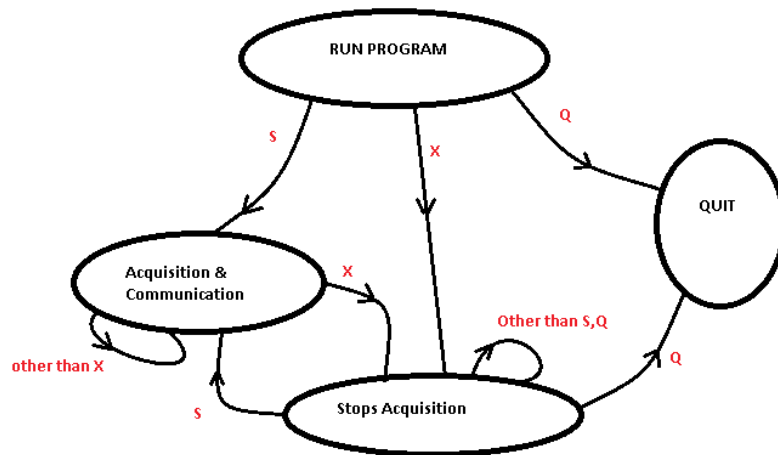

Fig. 9 State level transition diagram for the PC-Launchpad interface

The letters *S*, *X*, *Q* shown in Fig. 9 indicate the user inputs to the Interface program determining the transition between states. Based on the user input, the interface program communicates to the microcontroller whether to start the acquisition, to stop the acquisition, or to stop and quit the interface program.

System calibration

The EDR system was built with the external resistance $R = 220$ kΩ having a tolerance of +1%. The system was then tested by replacing R_{hand} with known resistances. Table 1 illustrates the calibration results.

Table 1. Calibration results using a known resistance in place of R_{hand}

R_{hand} used, Ω (±5% tolerance)	Measured value of R_{hand}, Ω (±100 Ω)	ADC output, *OUT* Hex (Decimal) value	Evaluated R_{hand}, Ω
Short Circuit (0)	0	0x000 (0)	0
100 k	99 k	0x13E (318)	99.0935 k
220 k	222 k	0x203 (515)	222.5933 k
1 M	1.009 M	0x348 (840)	1.0043 M
Open Circuit (∞)	∞	0x3FF (1023)	225 M

It is evident from Table 1 that the evaluated R_{hand} (last column) exhibits a negligible error compared to the known resistance used (second column). In case of larger deviation, the reference resistance *R* should be measured explicitly and used in calculations. Also, it has been observed that the system collects data at a rate of 152.34 + 1 samples/second.

Future improvements

In this project, an EDR sensor was based on the exosomatic measurements on the underlying assumption that the skin resistance is only changed by psychophysiological state of a subject and the applied voltage may not have severe impact. This can be a limitation in few cases that can, however, be overcome by making the sensor endosomatic using other (and more expensive) hardware. The latter can be achieved by implementing stages of OP-amps for amplification and signal conditioning. Also, the nonlinearity issue can be addressed, by

redesigning the sensor circuit and using an advanced ADC with a higher bit resolution. Safety of the system can be improved by isolating the EDR sensor's power source by including a separate battery-powered and regulated source.

Present system only operates at 9600 baud rate limited by the default driver available from Microsoft. By developing a new driver and communication circuitry as well as advanced ADC, the number of samples recorded per second can be increased. By using wireless daughter boards or extensions, such as CC110L RF Booster Pack [23] by Texas Instruments, the system can be made wearable and wireless and would have a smaller form factor.

Experimental results and discussions

Two experiments were conducted with the EDR system to study the effect of Visual Stimulation and Deep Breath on EDR. The subject was a healthy 22 year old male with no known psychophysiological disorders. EDR data have been collected using the designed system and stored on a PC for further analysis.

Visual stimuli

The subject was initially relaxed while sitting in a comfortable chair and asked to look at an animated picture. The stimulation included scary elements appearing suddenly in the middle of the animation, therefore, eliciting emotional activation in the subject [18]. The EDR data collected is shown in Fig. 10.
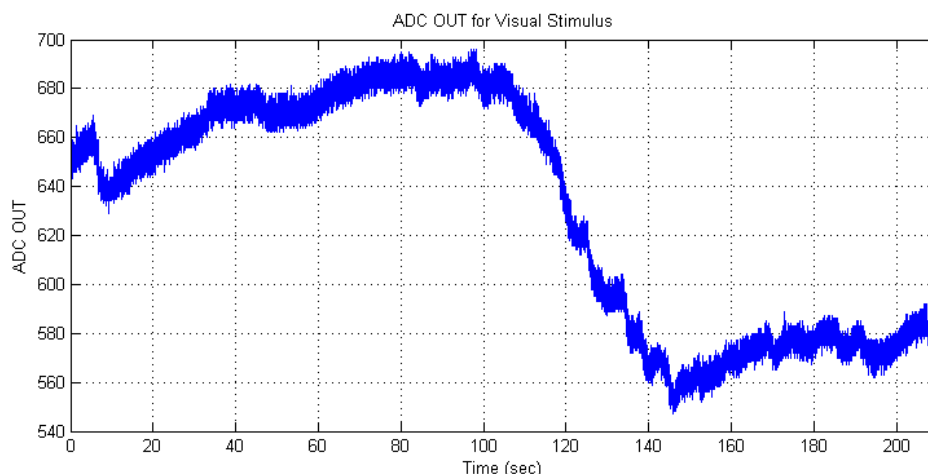

Fig. 10 ADC Output *OUT*, a measure of EDR, for visual stimulus

As seen in Fig. 10, the scary part of the visual stimuli might have emotionally activated the subject causing a dip in the EDR during seconds 100 to 150. Since the pictures were scary in nature, this emotional arousal can be attributed to negative valence. The ADC output *OUT* was used to evaluate R_{hand} using Eq. (4). The graph corresponding to R_{hand} of visual stimuli is illustrated in Fig. 11.
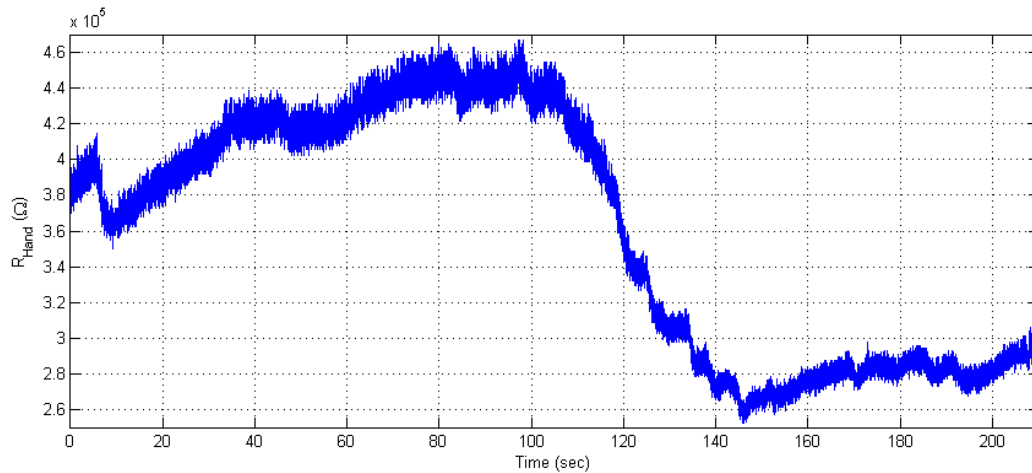
Fig. 11 R_{hand} as a function of time for visual stimulus experiment

We observe in Fig. 11 that R_{hand} has a similar pattern that of ADC Output *OUT* as observed in Fig. 10 and dropped approximately from 440 kΩ to 260 kΩ following the scary visual stimuli.

Deep breath
The subject was initially relaxed while sitting in a comfortable chair and asked to perform deep breath with a break of few seconds. The EDR data collected is illustrated in Fig. 12.
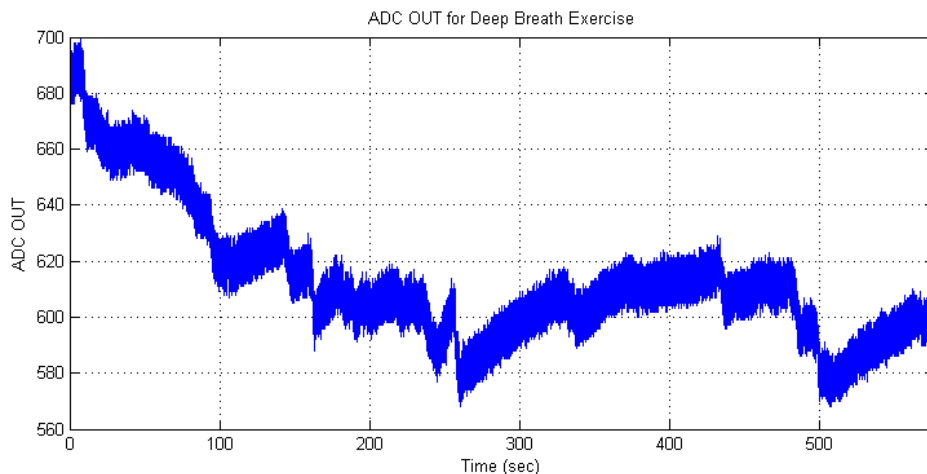

Fig. 12 ADC Output *OUT*, a measure of EDR, for deep breath exercise

As seen in Fig. 12, the deep breath exercise results in an increased sweat gland activity that reduces the skin resistance. The latter produces a dip in ADC output *OUT*, which is a measure of EDR, during the seconds 200-300 and also around the 500th second. As the subject was initially relaxed and took a deep breath, the EDR dip corresponds to a Positive valence based emotional activity and the same was confirmed by the subject. The ADC output *OUT* was used to evaluate R_{hand} using Eq. (4). The graph of corresponding R_{hand} in the deep breath exercise is illustrated in Fig. 13.
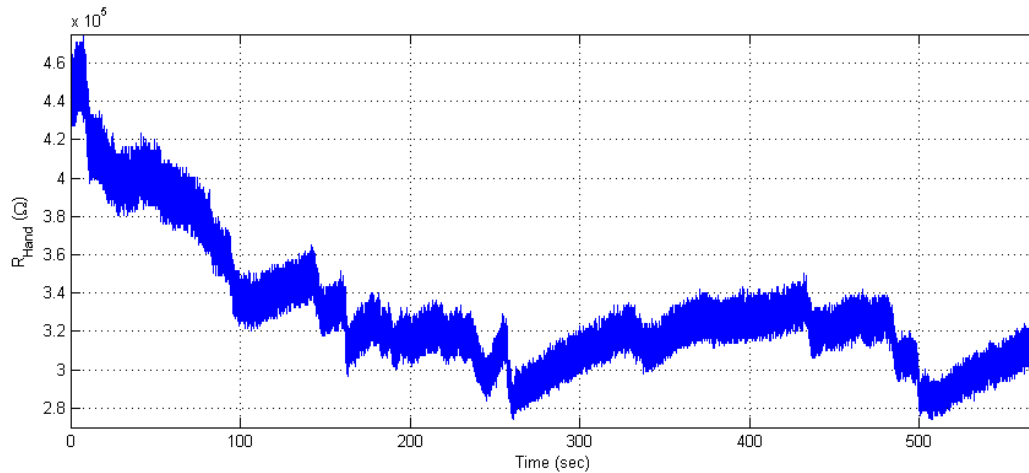
Fig. 13 R_{hand} as a function of time for deep breath exercise

We observe in Fig. 13 that R_{hand} has a similar pattern to that of ADC Output *OUT* as observed in Fig. 12.

Discussion

We observe that the graphs for the hand resistance R_{hand} are similar to ADC output *OUT* graphs, where both of them represent a measure of EDR. The range of R_{hand} in both experiments was from 270 kΩ to 480 kΩ that falls in the general EDR range of 50 kΩ to 1 MΩ [29].

From the Fig. 11 and 13, it is clear that both experiments have similar variation in EDR in terms of the range. When emotionally activated, R_{hand} took a dip from approximately 500 kΩ to 250 kΩ. On the other hand, the experiment with Visual Stimuli has negative valence and the experiment with Deep Breath has positive valence. This confirms the fact that EDR can be used to detect whether the subject is emotionally activated or not and cannot be used to detect the valence. Since both experiments were conducted on the same subject, the baseline of R_{hand} for the relaxed condition is quite similar in both cases and is at approximately 460 kΩ. This quantifies the designed system's precision.

In the results shown in Figs. 10-13, a presence of predominant local variations are evident. Generally, as the skin resistance doesn't change quickly [13], we can safely attribute the local variations to noise contaminations. A careful observation of Figs. 10 and 12 reveals that these local variations are approximately +/- 10 units of ADC OUT from the centre of signal at any point. One ADC OUT can be referenced to (V_{in} /1024 = 3.6/1024) 3.5 mV. The variation of 10 ADC OUT units can be approximated to a variation of 35 mV.

The noise in the EDR signal as shown in Fig. 14 is estimated as the difference between original signal and output of a simple moving average filter of order 100. Short time Fourier transform is applied on the noise estimate, using spectrogram function of Matlab, to obtain the spectral plot which is shown in the Fig. 15.

A faint yellow line highlighted in the black rectangular box in the Fig. 15 spans over the complete time, represents a normalized frequency of 0.7874 (f = 0.7874*fs/2 = 60.6298 Hz, where fs is approximately 154 samples/sec) which corresponds to the noise introduced by power line interference (which is from 60 Hz 120 V AC power supply to the PC that in turn powers the experimental Launchpad circuitry through USB). It is evident that a uniform random noise is present across all the frequencies. As we are measuring the skin resistance using a

potential divider circuit at room temperature, thermal noise which is a form of white noise have contaminated the signal. Also, another important source of contamination is from the measurement site itself in the form of skin potential which is in the range of 20-30 mV generally [13]. In this experiment, we have assumed the measured site to be a linear passive resistor but in reality it needs to be modeled as a nonlinear RC circuit with internal excitation [13].
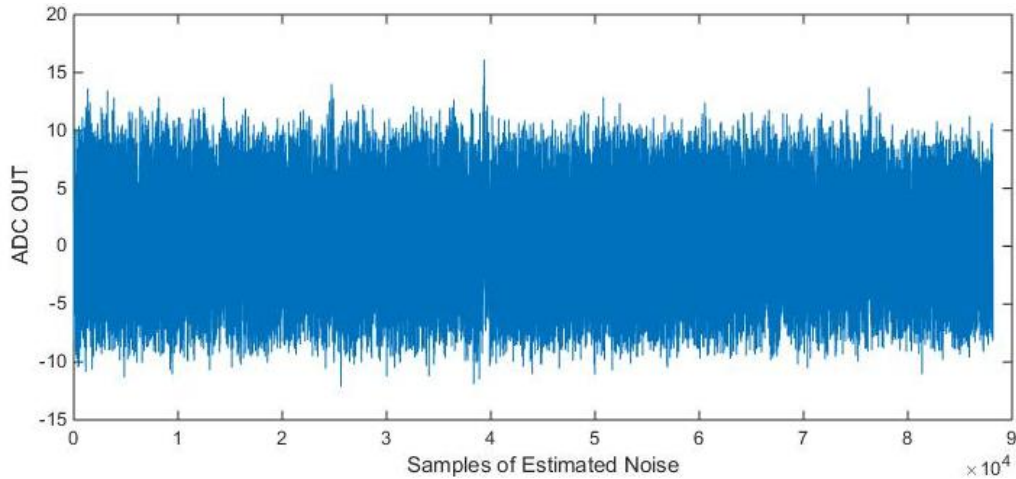

Fig. 14 Noise estimated as difference between deep breath experiment's ADC output *OUT* and its output of moving average filters of the order 100
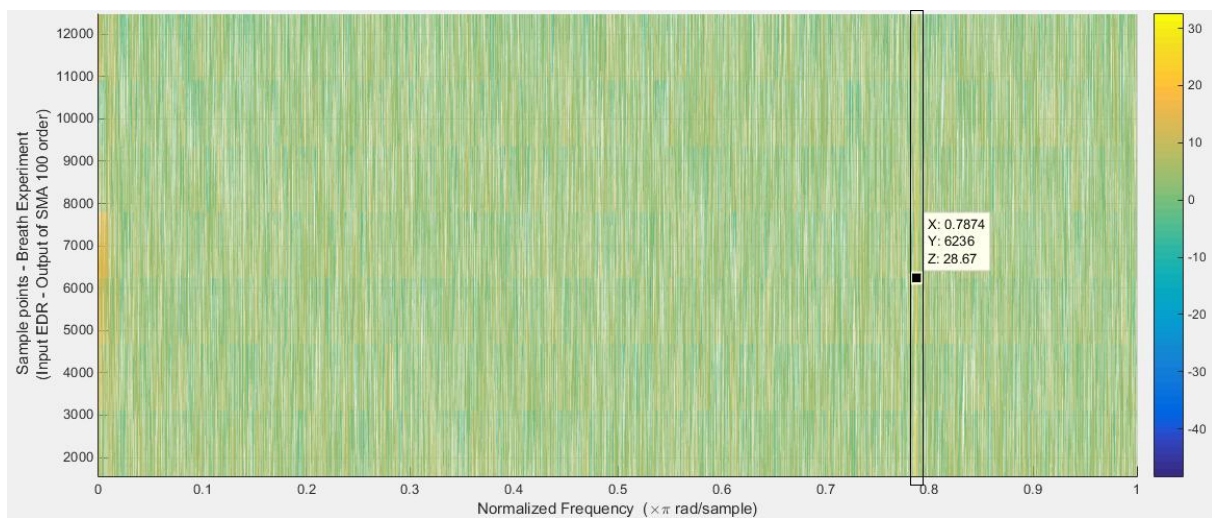

Fig. 15 Spectrogram plot of noise estimated (as shown in Fig. 14)

Even with the presence of the local noise, the observations and inferences made in our current experiment based on the electro-dermal response using skin resistance as a measurement are valid and true because the Skin resistance does not vary quick enough and has a normal operating range of 50 kΩ to 1 MΩ [29]. In our current experimental setup, this normal skin resistance range can be approximated to 190-840 ADC OUT units and in turn estimated to 0.665-2.940 V. The observed noise is estimated to have a peak-to-peak of 70 mV, i.e. 0.07 V. In the similar experimental setup, the noise immunity can be further increased by choosing the external series resistor with lower value instead of 220 kΩ by slightly foregoing the linear operational range corresponding to the R_{hand} range of 50 kΩ to 1 MΩ.

This local noise can also be reduced by using various low pass filters, for instance, a moving average filter acting as a low pass filter would suppress the high frequency noise. In this paper, a moving average filter was chosen, since such filters are simple to construct, efficient

in eliminating the local disturbances/noise, and determining the general trend when used with the proper order. Moving average filters of order 10 and 100 were applied to ADC output *OUT* of both experiments. The obtained results are shown in Fig. 16.
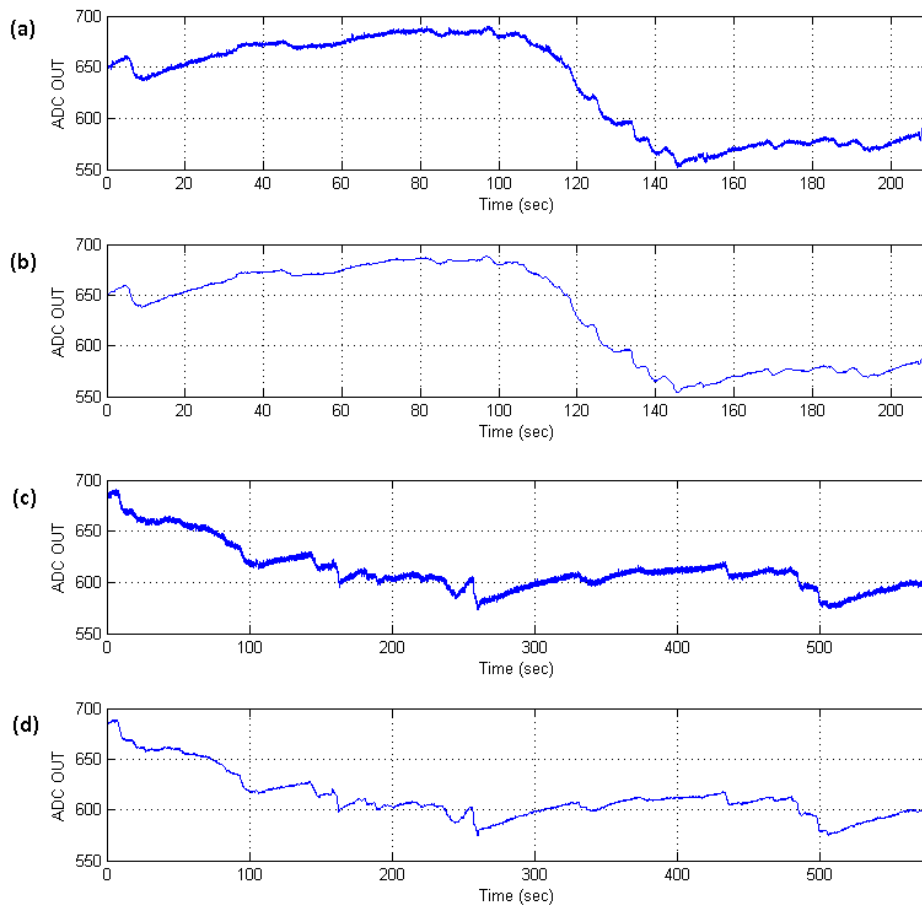

Fig. 16 Output of moving average filters of the orders 10 (a) and 100 (b) applied on the visual stimulus experiment ADC output *OUT*; output of moving average filters of order 10 (c) and 100 (d) applied on the deep breath experiment's ADC output *OUT*.

It can be seen in Fig. 16 that the local noise in the filtered output was decreased compared to the input signals. Also, as the filter order was increased from 10 to 100, the graphs indicated the decreased local noise and a smoother overall appearance. On the other hand, the sharpness in variations decreases too as the filter order was increased. Using a proper order for the moving average filter, filtered output can be more accurately used for identifying the temporal markers for drastic emotional variations compared to the raw EDR signal.

Conclusion

We conclude that the low cost TI MSP430 Value Line Launchpad kit may be used for measuring EDR with the precision sufficient for general applications. The proposed design implements exosomatic EDR estimation while using a general potential divider based EDR sensor. The recorded signal can be stored on a PC for a future analysis. The experimental results obtained with the system prototype were in the agreement with the theory and with the results reported previously. The experimental EDR data can be conditioned by applying a low pass filter to improve the accuracy of the system. Therefore, despite a few observed hardware and software limitations, the proposed low-cost EDR device may be implemented in various commercial applications and research fields.

References

1. Affectiva Inc, Q Sensor 2.0, http://qsensor-support.affectiva.com/, (Last accessed March 24, 2015).
2. Boucsein W. (2011). Electrodermal Activity, 2nd Ed., Springer Verlag.
3. Cacioppo J., L. Tassinary, G. Bernston (Eds.) (2007). Handbook of Psychophysiology, 3rd Ed., Cambridge University Press.
4. Fuller G. (1977). Biofeedback: Methods and Procedures in Clinical Practice, Biofeedback Press.
5. Grimmes S. (1982). Psychogalvanic Reflex and Changes in Electrical Parameters of Dry Skin, Medical and Biological Engineering and Computing, 20, 734-740.
6. Haag A., S. Goronzy, P. Schaich, J. Williams (2004). Emotion Recognition Using Bio-sensors: First Steps Towards an Automatic System, In: André E., L. Dybkjær, W. Minker, P. Heisterkamp (Eds.), Affective Dialogue Systems, Springer Berlin/Heidelberg, 36-48.
7. Handler M., R. Nelson, D. Krapohl, C. Honts (2010). An EDA Primer for Polygraph Examiners, Polygraph, 39, 68-108.
8. Joshi A., S. Ravindran, A. Miller (2011). EKG-based Heart-rate Monitor Implementation on the LaunchPad Value Line Development Kit Using MSP430G2xx, http://www.ti.com/lit/an/slaa486a/slaa486a.pdf, (Last accessed March 24, 2015).
9. Karjalainen P. (2012). Galvanic Skin Response (GSR), http://bsamig.uef.fi/research/gsr.shtml, (Last accessed March 24, 2015).
10. Kuncheva L., T. Christy, I. Pierce, S. Mansoor (2011). Multi-modal Biometric Emotion Recognition Using Classifier Ensembles, In: Mehrotra K., C. Mohan, J. Oh, P. Varshney, M. Ali (Eds.), Modern Approaches in Applied Intelligence, Springer Berlin / Heidelberg, 317-326.
11. Lichtenstein A., A. Oehme, S. Kupschick, T. Jürgensohn (2008). Comparing Two Emotion Models for Deriving Affective States from Physiological Data, In: Peter C., R. Beale (Eds.), Affect and Emotion in Human-computer Interaction, Springer Berlin/Heidelberg, 35-50.
12. Liechti C. (2012). pySerial, http://pyserial.sourceforge.net/, (Last accessed March 24, 2015).
13. Malmivuo J., R. Plonsey (1995). Bioelectromagnetism: Principles and Applications of Bioelectric and Biomagnetic Fields, Oxford University Press, New York.
14. Neumann E., R. Blanton (1970). The Early History of Electrodermal Research, Psychophysiology, 6, 453-475.
15. Nicolaou M. A., H. Gunes, M. Pantic (2011). Continuous Prediction of Spontaneous Affect from Multiple Cues and Modalities in Valence-arousal Space, IEEE Trans Affective Comput, 2, 92-105.
16. Poh M.-Z., N. Swenson, R. Picard (2010). A Wearable Sensor for Unobtrusive, Long-Term Assessment of Electrodermal Activity, IEEE Transactions on Biomedical Engineering, 57, 1243-1252.
17. Python Software Foundation, Python, https://www.python.org/, (Last accessed March 24, 2015).
18. Scary Optical Illusion, http://www.eyetricks.com/scary_optical_illusion2.htm, (Last accessed March 24, 2015).
19. Scerbo A. S., L. W. Freedman, A. Raine, M. E. Dawson, P. H. Venables (1992). A Major Effect of Recording Site on Measurement of Electrodermal Activity, Psychophysiology, 29, 241-246.
20. Schwartz M., F. Andrasik (Eds.) (2003). Biofeedback: A Practitioner's Guide, 3rd Ed., The Guilford Press, 2003.

21. Sheperd P. (2012). The Emotional Response Indicator, http://www.trans4mind.com/transformation/gsr.htm, (Last accessed March 24, 2015).
22. Storm H., K. Myre, M. Rostrup, O. Stokland, M. D. Lien, J. C. Raeder (2002). Skin Conductance Correlates with Perioperative Stress, Acta Anaesthesiologica Scandinavica, 46, 887-895.
23. Texas Instruments Inc., CC110L RF BoosterPack, http://www.ti.com/tool/430boost-cc110l, (Last accessed March 24, 2015).
24. Texas Instruments Inc., MSP430 LaunchPad Value Line Development Kit, http://www.ti.com/tool/msp-exp430g2, (Last accessed March 24, 2015).
25. Texas Instruments Inc., MSP430G2x31 MSP430G2x21 Mixed Signal Controller Datasheet, http://www.ti.com/lit/ds/symlink/msp430g2231.pdf, (Last accessed March 24, 2015).
26. Texas Instruments Inc., MSP430x2xx Family User's Guide, Texas Instrument Inc, http://www.ti.com/lit/ug/slau144j/slau144j.pdf, (Last accessed March 24, 2015).
27. Valenza G., A. Lanata, E. P. Scilingo (2011). The Role of Nonlinear Dynamics in Affective Valence and Arousal Recognition, IEEE Transactions on Affective Computing, 3(2), 237-249.
28. Wang P., H. McCreary (2006). EDA Sensor, https://courses.cit.cornell.edu/ee476/FinalProjects/s2006/hmm32_pjw32/index.html, (Last accessed March 24, 2015).
29. Westland J. C. (2011). Electrodermal Response in Gaming, Journal of Computer Networks and Communications, 2011, 1-14.
30. Wikipedia Contributors, Skin Conductance, http://en.wikipedia.org/w/index.php?title=Skin_conductance&oldid=485989510, (Last accessed March 24, 2015).

Sumanth Reddy Yeddula, M.Sc.
E-mail: sumanthreddy.y@gmail.com

Sumanth Reddy Yeddula received his Bachelor of Technology in Electrical and Electronics Engineering from Sri Venkateswara University College of Engineering, Tirupati (A.P-517502), India in 2006. He also received his M.Sc. from Lamar University, Beaumont, TX, USA in 2012.

Assoc. Prof. Gleb V. Tcheslavski, Ph.D.
E-mail: gleb@lamar.edu

Gleb V. Tcheslavski has received his Engineer degree from Bauman Moscow State Technical University and Ph.D. in Electrical Engineering from Virginia Tech. He is with Drayer Department of Electrical Engineering, Lamar University serving as an Associate Professor.